Blast wave propagation into the brain

Jan Arild Teland and Morten Huseby

Norwegian Defence Research Establishment (FFI)

7 December 2012

FFI-rapport 2012/02416

119301

P: ISBN 978-82-464-2181-0
E: ISBN 978-82-464-2182-7

Emneord

Sjokkbølge

Hjerneskade

Numerisk simulering

IED

Godkjent av

Eirik Svinsås	Prosjektleder
Jan Ivar Botnan	Avdelingssjef

English summary

Military personnel are exposed to blast waves during training and combat. IED's (Improvised Explosive Devices) have for some time caused more fatalities than other threats for Norwegian soldiers, and there have also been cases of close-in detonation without fatalities. This report addresses damage to the brain as a result of a blast wave propagating through it. International experience indicates that such damage can occur at relatively small pressure levels. Even at levels occurring in peace time training with heavy weapons, the brain is affected by the same mechanisms, leading to small hemorrhages in brain tissue. Even if blast waves induced in training does not lead to TBI (Traumatic Brain Injury), the long term effects of repeated exposure is not known.

This work tries to shed light on the underlying mechanisms that lead to both TBI from IEDs and mTBI (mild Traumatic Brain Injury) from training. This is done by numerical simulation of propagation of blast waves through the skull and brain, as well as taking advantage of data from animal experiments performed by other groups.

First we validate our numerical method by performing 2D simulations of blast wave propagation inside a pig head and comparing with actual pressure measurements in pig brains. Then we apply 3D simulations to examine the response of the human brain to blast waves from different sources, including 155 mm artillery, 12.7 mm rifle and a moderate sized IED of 7.5 kg homemade explosives located at 4.5 meter distance.

The various simulations provided new insight into the nature of blast wave propagation into the brain. The blast wave was seen to propagate into the brain directly through the skull bone with the general size and shape of the blast wave mostly unaffected by openings in the bone (nose, ears, eyes, throat). Thus, the skull bone does not offer much protection to the brain. However, the orientation of the head relative to the blast wave was seen to have a huge effect on the pressure distribution inside the brain. In general the full 3D results were consistent with the 2D results.

We now have a validated numerical method for studying the pressure propagation, and other physical parameters, inside a human head exposed to a blast wave. This could be useful in further exploring the mechanisms that possibly lead to brain injury, both from "weak" shock waves from weapons and from "strong" shock waves from an IED.

Sammendrag

Militært personell utsettes for sjokkbølger både under trening og kamp. IED'er (Improvised Explosive Devices) har i en periode ført til flere dødsfall for norske soldater, og det har også vært en rekke hendelser med "nærkontakt". Denne rapporten ser på hjerneskade som følge av sjokkbølger. Internasjonal erfaring tyder på at slik skade kan skje selv ved relativt små trykk. Til og med ved trykknivåer som soldatene utsettes for ved trening med tunge våpen i fredstid, påvirkes hjernen av samme fysiske mekanismer, noe som kan føre til små blødninger i hjernevevet. Selv om dette ikke fører til TBI (Traumatic Brain Injury), så er langtidseffektene av gjentatte slike påvirkninger ukjent.

Dette arbeidet prøver å kaste lys over de underliggende mekanismene som fører til både TBI fra IED'er og mTBI (mild Traumatic Brain Injury) fra trening. Dette gjøres ved numeriske simuleringer av propagasjon av sjokkbølger gjennom hodeskallen og hjernen, samt ved å utnytte data fra dyreforsøk utført av andre grupper.

Vi validerer først den numeriske metoden ved å utføre 2D-simuleringer avsjokkbølger som propagerer inn i en grisehjerne og sammenligne med faktiske målinger. Deretter bruker vi 3D-simuleringer til å undersøke responsen til en menneskehjerne på sjokkbølger fra forskjellige kilder, inkludert 155 mm artilleri, 12.7 mm rifle og en IED av moderat størrelse (7.5 kg HME (hjemmelaget eksplosiv) på 4.5 meters avstand.

De forskjellige simuleringene gav oss ny innsikt i hvordan sjokkbølger propagerer inn i hjernen. Vi så at bølgen ble overført til hjernen direkte via hodeskallen og at sjokkbølgens form stort sett var uavhengig av hodeskallens åpninger (nese, øyne, ører etc). Hodeskallen gir derfor ikke noen særlig beskyttelse mot sjokkbølger. Imidlertid hadde hodets orientering i forhold til sjokkbølgen stor effekt på trykkfordelingen i hjernen. Generelt var resultatene fra 3D-simuleringene konsistente med 2D-resultatene.

Vi har dermed en validert numerisk metode for å studere trykkpropagering, og andre fysiske parametere, i et menneskehode som utsettes for en sjokkbølge. Dette kan være nyttig for å videre utforske mekanismene som muligens fører til hjerneskade, både fra "svake" sjokkbølger fra våpen eller "sterke" sjokkbølger fra en IED.

Contents

1 Introduction

Military personnel are exposed to blast overpressure during training and combat. IED's (Improvised Explosive Devices) have for some time caused more fatalities than other threats for Norwegian soldiers. Soldiers experiencing an IED attack may be injured or killed by the forces or lethal pressure they may experience when their vehicle is hit. Dismounted soldiers may be hit by fragments. An injury that is harder to acknowledge is damage to the brain as a result of a blast wave propagating trough it. There is evidence that such damage can occur at relatively small pressure levels (1). Even at levels occurring in peace time training with heavy weapons or explosives, the brain can be affected by the same mechanisms leading to small hemorrhages in brain tissue. Even if blast waves induced in training does not lead to TBI (Traumatic Brain Injury), the long term effects of repeated exposure is not known (2).

Blast induced TBI is a field containing numerous unsolved questions that will take the scientific community time to resolve. This work tries to contribute to the solution of one of these problems, the underlying mechanisms that lead to both TBI from IEDs and mTBI (mild Traumatic Brain Injury) from training. This is done by numerical simulation of the propagation of the blast waves through the skull and brain as well as taking advantage of data from animal experiments performed by other groups.

This report summarises the work done at FFI on blast wave injury to the brain. Some of it has been performed in cooperation with Gøteborg University. Part of the work has already been published externally (3,4) but is included here for completeness.

The report is divided into four main parts:

1. Description of observed damages to the pig brain at moderate blast waves, where test pigs were anaesthesized and then exposed to blast waves from firing of heavy weapons. This is the same pressure levels that military personnel are regularly exposed to during training. The pressure was measured in the brain of the pigs, and the brain was sliced to look for damages. We also describe the reduced cognitive level of rats exposed to the same blast waves.
2. Validation of the simulation methods against pressure measurements in the brain of the pigs. In the context of this paper, the main result is to validate the simulation methods against measurements.
3. Simulation of blast waves propagating through a human brain with 3D geometry. To obtain experimental data for the pressure in the human brain, caused by the blast wave, is not possible. Thus validation with pig data is the best that can be obtained. Still, the goal of this work is to draw conclusions that are relevant for blast wave exposure to the human brain. We set up some simulations to that end, highlighting important aspects of blast wave propagation through the human brain.
4. Simulation of blast wave from a moderate sized IED propagating through a 3D model of the human head. This corresponds to pressure levels that would not lead to lung damage, but would probably rupture the unprotected eardrum.

2 Pig experiments

Exposure to low levels of blast in a shock tube impairs the performance of rats in cognitive tests, indicating a potential effect also for humans. In another animal experiment (5), pigs were placed in crew position relative to large caliber weapons to simulate military training scenarios. After exposure, microscopical evidence for small hemorrhages in the brain tissue and signs of brain edema were found in the pigs. In these experiments, the maximal peak value of the blast (P_{max}) recorded in the pig´s brain was comparable with that in air outside the head. These results suggest that the skull bone offers little protection for the brain against blast. The study did not explore the mechanisms for blast wave propagation into the brain, nor the importance of geometrical and material parameters of the skull bone.

Anesthetized pigs were placed in the gunner´s position of the AG90 or FH77 and received 3 consecutive exposures (Fig. 2.1). The pressure, as a function of time, was recorded during blast exposure, both inside the brain and in air 10 cm from the head of the animal. The air recording reflects the free field pressure fairly well, since the pressure sensor is located far enough away from the head to make surface reflections insignificant. A hydrophone (diam. 9.5 mm, model 8100; Brüel &Kjær) or a pen-shaped piezo-electric sensor (PCB 137A23) were used for the recordings in air. Hydrophones were routinely used as pressure sensors in the pig brain (Figure 2.2).

Figure 2.1 Position of pigs in animal experiments (FH77 in the middle, AG90 to the right).

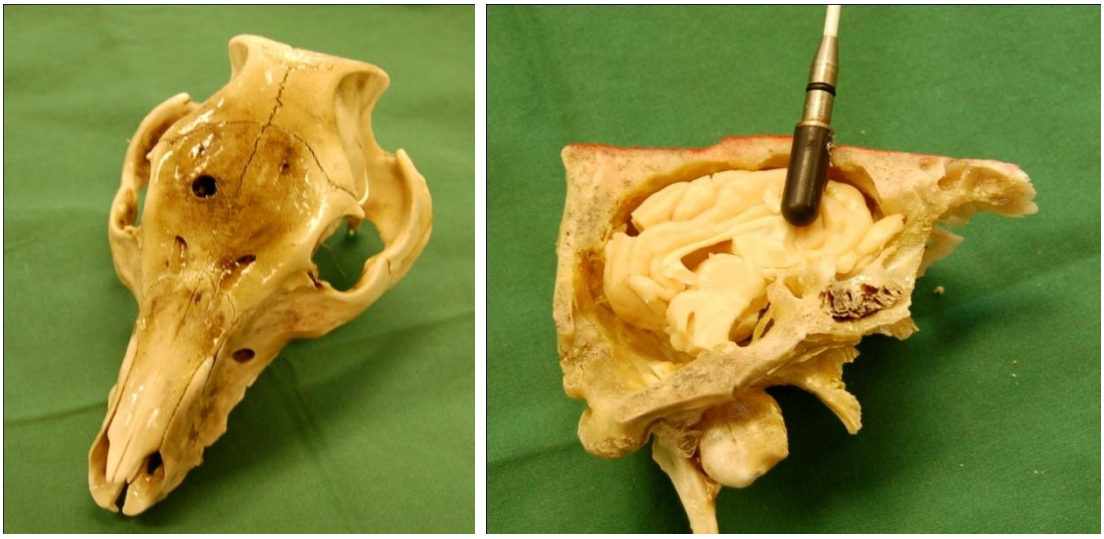

Figure 2.2 The pig skull and brain and location of the pressure gauge.

The measurements showed that the maximum pressure amplitude recorded in the brains was of similar or slightly reduced magnitude compared to the free field pressure (Figure 2.3). The contribution of head acceleration to injury induction was determined with high-speed video and an accelerometer, which was aligned with the axis of impact and attached to the animal´s head. At the levels of blast overpressure used in our experiments, the mean acceleration of the head was very small and not considered to be causative to the measured pathophysiologic and functional changes.

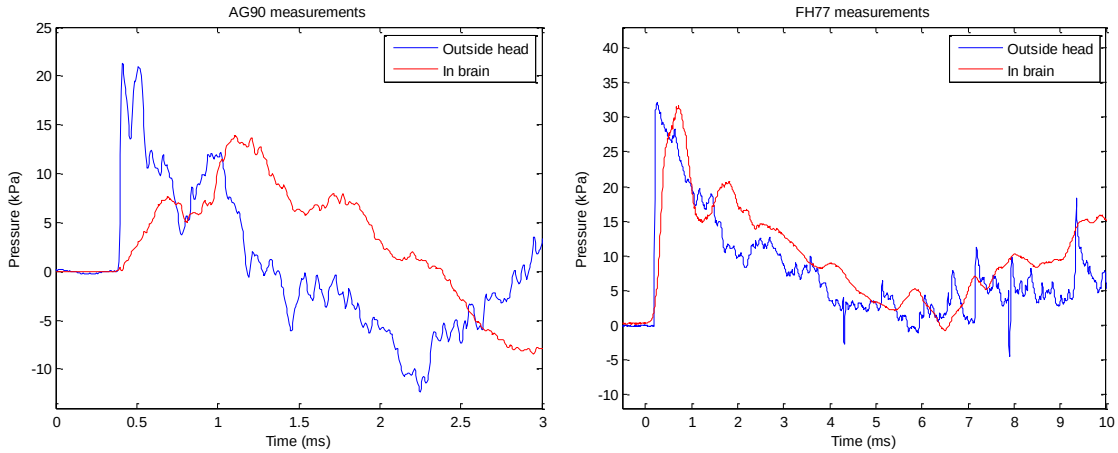

Figure 2.3: Pressure recordings inside pig brain and outside head after firing of an AG90 (left) and FH77 (right).

3 Numerical method

To validate the simulation methods against measurement data we simulated pressure waves propagating through a pig head. This was done with a simplified geometry, assuming axis-symmetry, i.e. 2D-simulation. In addition we assume front-rear symmetry. One reason for this choice is that good geometry data for the brain are harder to find for pigs than for humans.

Another reason is that 2D-simulations are a lot quicker to carry out. This made it possible to carry out extensive testing and parameter studies.

Assuming an axially symmetric head, this could also be modelled in 2D. However, the head must then be situated along the axis of the gun barrel, thus either in front of the barrel or behind it. A position, say at some distance from the barrel at an angle of 90 degrees, is not possible to model without going to 3D. Fortunately, a position of the head right behind the barrel is very typical for a shooter, so this looks like a relevant test case which has the benefit of allowing 2D modelling. Thus, in our first 2D-approach we modelled a head placed behind the gun barrel.

3.1 The AUTODYN hydrocode

In numerical simulations of a physical system, the geometry of the situation is frequently divided into a number of elements. These elements are then given mathematical properties corresponding to the behaviour of the materials they model. During a simulation, time is discretized into time steps and the physical laws are applied to each element during each time step. Their state is then updated, for instance that the velocity, pressure or shape is changed and the same process is performed during the next time step[1]. Several commercial (and non-commercial) computer programs (often called hydrocodes) exist for performing such calculations.

ANSYS AUTODYN (6) is an explicit hydrocode for modelling rapid non-linear phenomena. It has a number of numerical processors or solvers, including Lagrange, Euler and SPH. It can handle both structured and unstructured meshes as well as combinations of the various numerical processors in the same problem.

AUTODYN has a number of numerical processors or solvers, including Lagrange, Euler and SPH. It can handle both structured and unstructured meshes as well as combinations of the various numerical processors in the same problem.

3.2 Lagrange processor

Perhaps the most common method for modelling a solid object is to use a Lagrangian processor[2]. This means that one defines various so-called nodes, which constitute a grid describing the geometrical object it models. This is typical for objects which initially have a specific shape and which are not expected to deform very much during the process under study. If the object is deformed, the location of the nodes changes and the grid takes a (slightly) different shape showing the new geometry of the object. This process is illustrated in Figure 3.1.

[1] The discretization in time steps is not always relevant, of course. In engineering problems, it may be of larger interest to calculate the equlibrium state under static loads. In such cases different methods are employed, even though a geometrical mesh is still used.

[2] A processor usually denotes an implementation of an algorithm based on a mathematical method in a specific computer code. The term "solver" is also frequently used.

A problem with the Lagrange processor is that the grid of highly deformed objects may become entangled, thus making it impossible to proceed with the simulation.

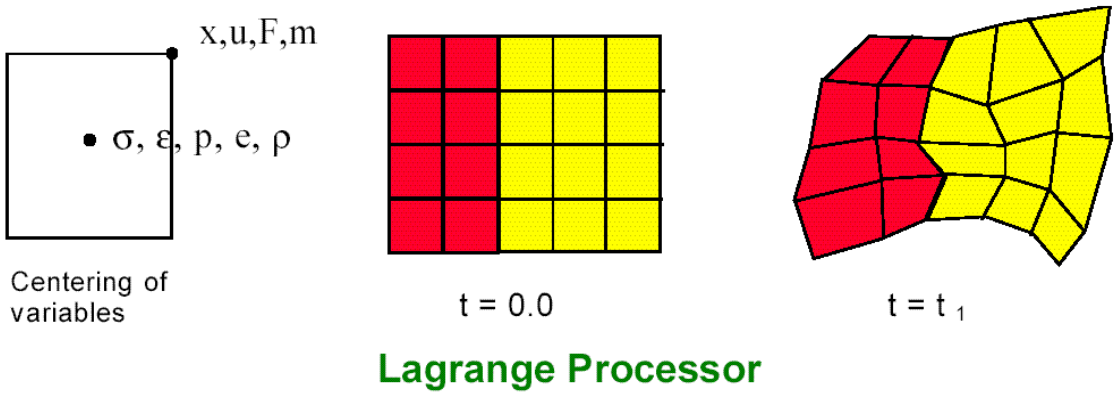

Figure 3.1 Illustration of the Lagrange processor.

3.3 Euler processor

Another option is the Eulerian processor. In this case one defines a grid that is fixed in space. This grid is then filled with material and during the physical process the material may flow between the elements of the grid while the grid remains constant. The process is depicted in Figure 3.2. The Euler processor is typically used for problems involving fluids and gases, as these do not have a specified initial shape.

Since the grid is constant, the Euler processor does not suffer from the problem of grid entanglement. However, the Euler technique has problems with tracking the surface of a solid object, as well as being more time and CPU expensive.

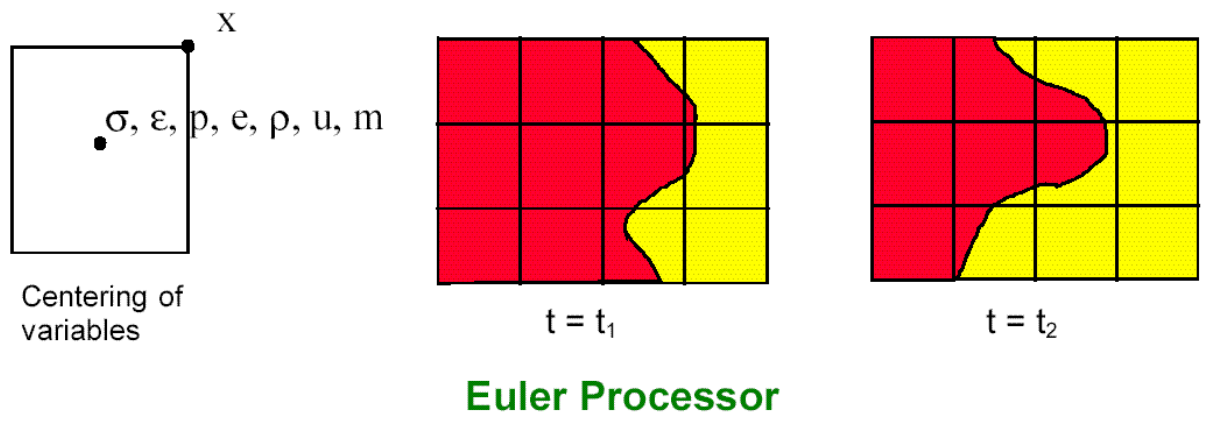

Figure 3.2 Euler processor.

AUTODYN has two different Euler solvers, Euler-FCT and Euler Multimaterial. The practical difference is that Euler-FCT is faster and more accurate, but only one material can be used in the simulation. Euler Multimaterial is slower and less accurate, but several materials may be present

in the grid. Thus, for our purposes, where the grid will contain both air and powder gas, Euler Multimaterial is the natural choice.

3.4 ALE

ALE (Arbitrary Lagrange-Euler) is an extension of the Lagrange processor. The difference is an additional computation step at each cycle, where the grid is redefined and the numerical solution is mapped onto the new grid using Eulerian techniques. There are several options available to the user on how this is achieved. If the simulation involves large deformations, an ALE grid will often proceed further than a pure Lagrange grid before stopping due to grid entanglement.

3.5 Meshing

Meshing is the process of creating a grid to model a specific situation. AUTODYN has various types of pre-processor tools to facilitate meshing. However, for generation of a 3D Euler grid, the only option is to use rectangular elements, whereas in 2D there are various other possibilities.

To create more complex non-rectangular structures in an Euler grid, it is possible to first define a Lagrangian "fill" subgrid and subsequently map it into the rectangular Euler grid.

If no boundary conditions are imposed on the edge of the Euler grid, it will by default act as a rigid boundary. Thus, any material pushed towards the boundary will not flow out, but will instead experience the edge as an infinitely rigid barrier. All waves reaching the boundary will therefore be perfectly reflected. It is also possible to define "unused" cells inside the grid, which will then work in the same way as the grid boundary, i.e. perfectly reflecting.

In the latest AUTODYN versions, it has become possible to import geometry from CAD into AUTODYN, thus making geometry modelling much simpler.

3.6 Material modelling

A material model is a mathematical relationship that defines how a material responds to various types of loading and external influences. To set up a problem in AUTODYN (or any other hydrocode), a material model must be provided for each material involved. Obtaining a good material model for a particular material is often very difficult, either because experimental data is not available, or the material has such a complex behaviour that only a small fraction of the necessary data can be captured in controlled experiments. AUTODYN contains a large material library of material models of varying quality.

In our case, we will need material models for air, powder gas and the materials present in the human or animal head. Fortunately, air and the powder gas are very simple to model using the ideal gas equation of state. An air model is included in the AUTODYN material library. However, modelling the human or animal head sufficiently accurate is much more challenging, and this will be discussed in detail later.

3.7 Numerical source

In this work our aim was to study the propagation of a blast wave produced by a weapon as it propagates into the brain of a pig placed in the shooter's position. Previously (7,8), the blast wave from a weapon has been simulated by first modelling the interior ballistics in IBHVG2 (9) and then the blast wave propagation as the gun powder gas escapes from the muzzle, using AUTODYN. This approach could in principle be applied in the present study, but would require very fine numerical grid resolution and possibly full 3D to capture the effects of the muzzle device on the weapon. However, since our objective was mainly to study the physics of the wave propagation, a simpler method could be adopted.

As a first approach the measured time series of the pressure wave from the relevant weapons was approximated with numerical blast waves from spherical detonations, which can be modelled in 1D. More precisely we use spheres of compressed air (at TNT energy and density) with radiuses 18 mm and 84 mm, respectively at distances of 2050 mm and 7700 mm. These give good approximations of the AG90 and FH77 blast waves, as shown in Figure 3.3. Although some details are lost, the most important aspects, like amplitude and duration, are captured.

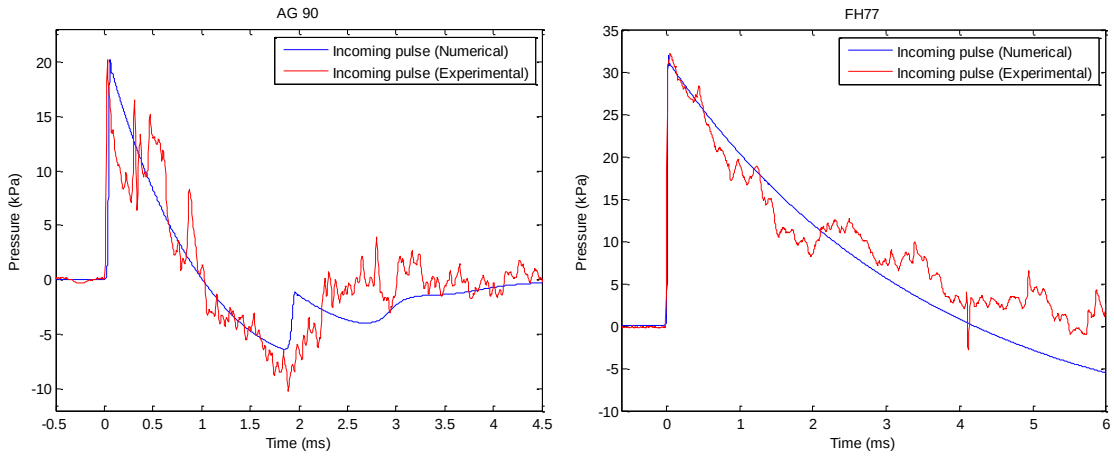

Figure 3.3 Comparison between measured free field blast wave and numerical simulations for AG90 and FH77.

3.8 Head modelling

The head of a human or animal contains many elements and is a quite complicated structure. However, in this investigation we are mainly interested in the physical mechanisms with regard to penetration of the pressure waves into the brain, so a simpler model will be sufficient. It will therefore first be assumed that the head consists of only two materials: skull bone and brain.

To save computation time and allow a finer numerical mesh, our first simulations are performed in 2D with axial symmetry. The skull is modelled as an outer elliptical surface with constant thickness of 5 mm, major radius of 43.5 mm and minor radius of 31 mm. The brain is modelled as a solid ellipse with major radius of 38.5 mm and minor radius 26 mm. This corresponds roughly to the actual pig head geometry.

Initially, the skull is modelled without holes, i.e. the openings for nervous tissue (spinal cord, optic nerve, olfactory nerve) and the large blood vessels. The head is modelled using one Lagrangian mesh for both the brain and bone material. This is justified since there is no vacuum or open spaces between the brain and skull and no sliding between surfaces is expected. The cell length in the Lagrangian mesh is roughly 1.5 mm. The area around the head is modelled using the Euler Multimaterial processor with a cell length of 1.0 mm in the area of interest. Gauge points for logging physical variables were placed at regular intervals in the air outside the head and inside the skull and brain (Figure 3.4). A limited sensitivity study of the mesh size was performed, indicating that the results were not particularly mesh sensitive and that a mesh resolution of 1.0-1.5 mm was quite sufficient.

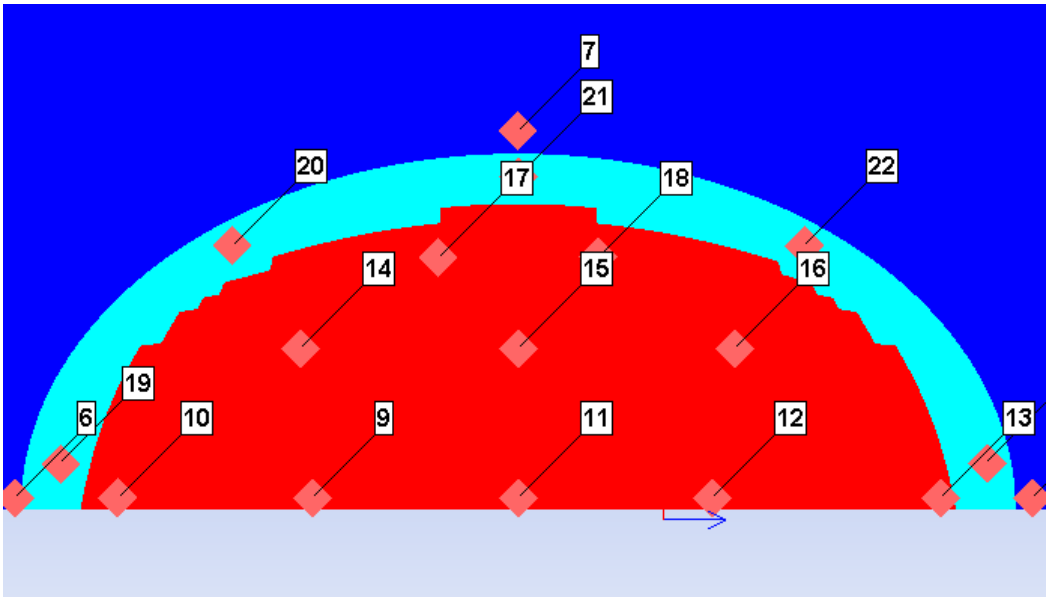

Figure 3.4 Pig head geometry with numerical gauge locations. The pressure wave travels from left to right. The brain is red, the skull light blue and the surrounding air is dark blue. The numbers show the positions of the various numerical gauges.

3.9 Material data

Having specified the geometry, we now need to define the material models for bone and brain. The skull is likely to remain elastic during all kinds of blast exposure from regular weapons. While the skull may fracture or become plastic from an impact, this does not happen from a blast wave with the amplitudes used here. A blast wave that could cause a fracture of the skull must be so massive that it will cause death with 100% certainty. Thus, plastic deformation is of no relevance at "weak" blasts that may or may not induce long-term injuries. Therefore, we can use a pure elastic model for the bone, simplifying things as we only need to specify the density and two elastic parameters.

Table 3.1 Skull and brain material parameters.

	Density (g/cm^3)	Bulk modulus (GPa)	Shear modulus (GPa)
Skull	1.90	7.80	3.51
Brain	1.04	2.30	0.24

The skull consists of two types of bone, centrally, the softer cancellous bone, demarcated by the harder cortical bone towards the inner and outer surfaces. From the viewpoint of mechanical modelling, these two bone types have properties that are reasonably similar (10) and will be treated as a single material. In reality, the bone is also slightly anisotropic i.e. with different elastic moduli for different directions, but for simplicity isotropic elasticity has been assumed. The skull parameters, shown in Table 3.1, are similar to the parameters used for human bone model in (11).

We used a pure elastic model for the brain as well, with a very low shear modulus to account for the brain being nearly incompressible. The selected parameter values are again quite similar to the human brain data used in (11), except that they used a viscoelastic model with a varying G-modulus.

4 Simulation AG90

The numerical results for AG90 were plotted for two gauge points, gauge #9 corresponding roughly to the location of the sensor in the animal experiment and gauge #11 in the center of the brain (Figure 4.1). We note that they are roughly consistent with the measurements (Figure 2.3) in that pressure amplitude inside the brain is slightly lower than in the air outside. The agreement is good taking into account all the simplifications made in the model.

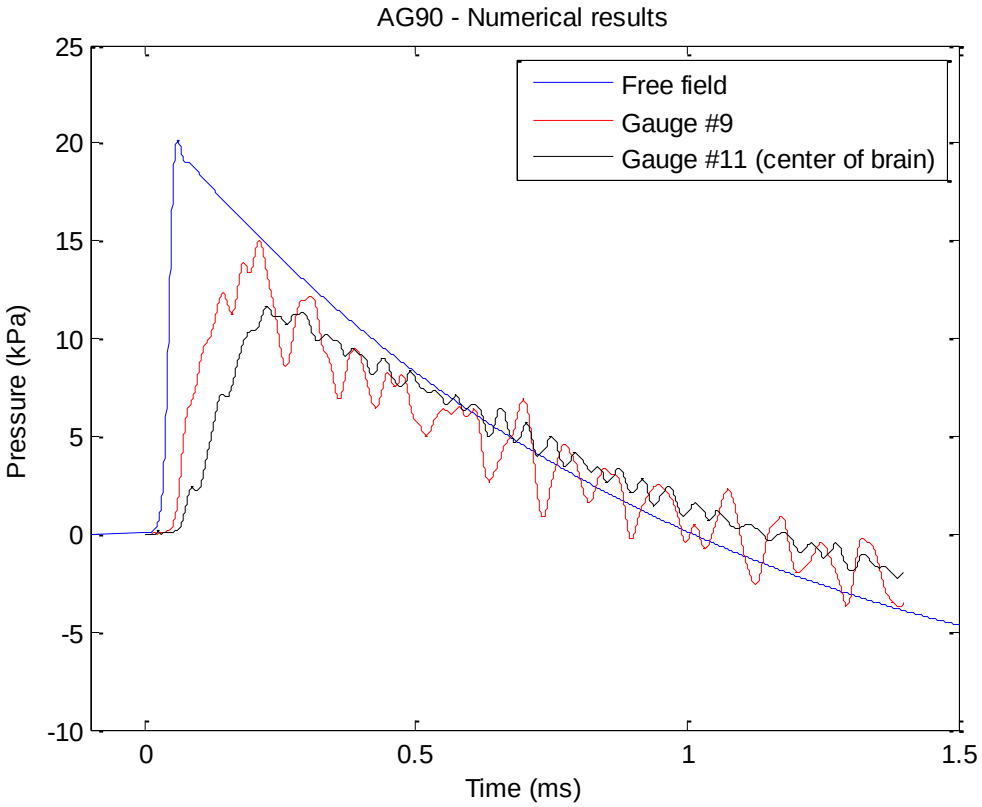

Figure 4.1 AG90 – Comparison of pressure history for the free field and inside the brain

In Figure 4.2 we show the pressure contour plots for the AG90 case as the blast wave passes the model pig head. The peak pressure was higher in the region of the brain facing the incoming blast wave, but still the blast wave propagates through the brain and skull creating significant amplitudes in all areas.

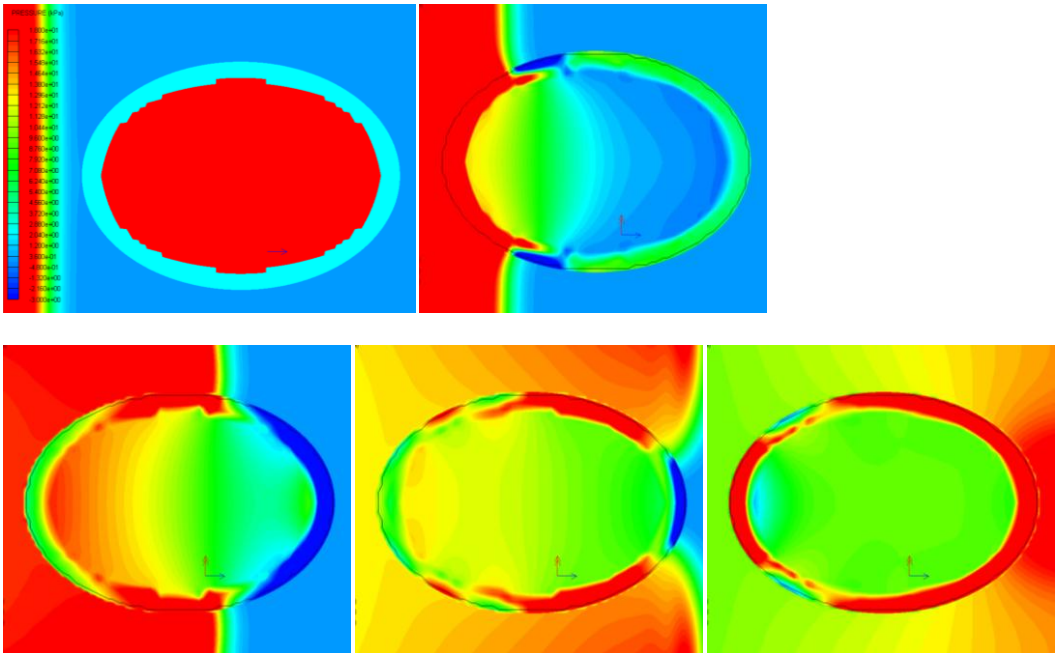

Figure 7 AG90 – pig head pressure contours at t=0.0 ms, 0.3 ms, 0.6 ms, 0.9 ms and 1.2 ms. Pressure scale is shown upper left.

5 Simulation FH77

The corresponding numerical results for the FH77 case are shown in Figure 5.1.

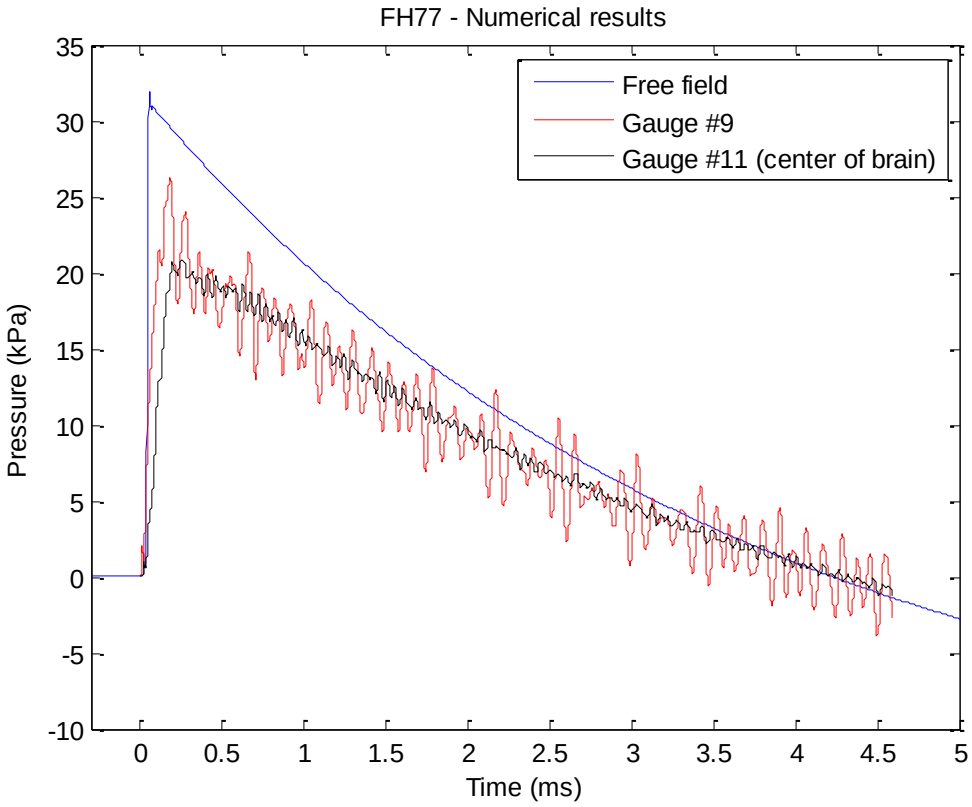

Figure 5.1 FH77 – Comparison of free field pressure and pressure inside the brain.

The various contour plots for the pig head in the FH77case are shown in Figure 5.2. The pressure distribution inside the brain is slightly different from AG90 because of the much longer duration of the incoming blast wave.

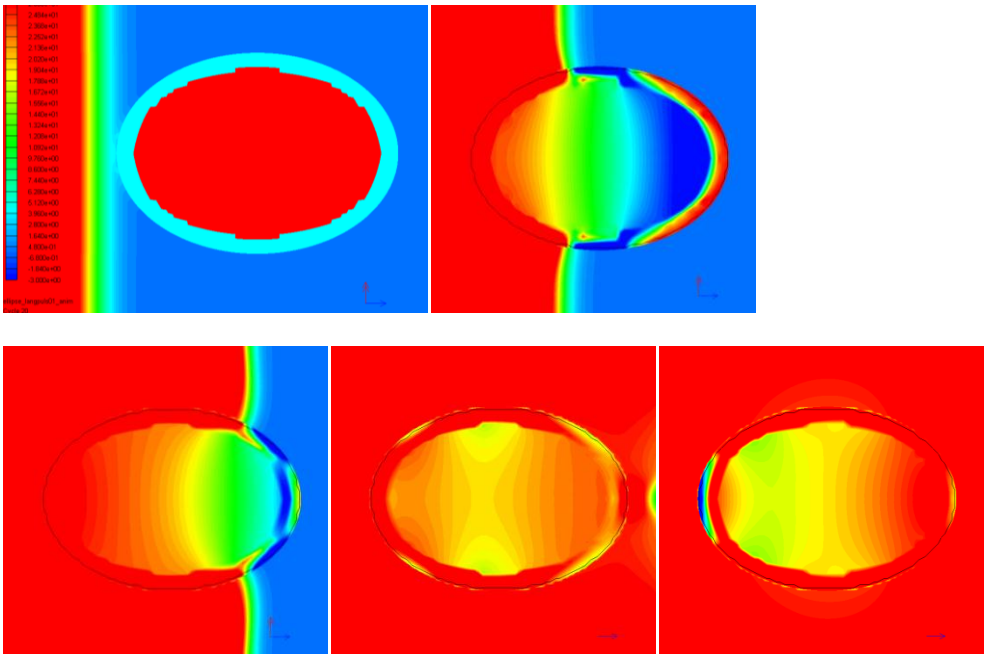

Figure 5.2 FH77 – pig head pressure contours at t=0.0 ms, 0.3 ms, 0.6 ms, 0.9 ms and 1.2 ms. Pressure scale is shown upper left.

6 Mechanisms of blast-wave propagation

The results indicate that our simple numerical model provides reasonably accurate results for the pressure measurements inside the brain. To investigate the phenomenon of blast wave propagation into the brain more closely, sensitivity studies were performed to examine the effect of various parameters on the brain pressure caused by a blast wave.

An interesting question is how the blast wave propagates into the brain, whether through the existing openings in the skull or directly through the bone tissue. The results so far have shown that the blast wave does propagate into the brain despite our model does not include openings. To investigate whether openings would have had any effects on the pressure in the brain, we have performed a simulation with a 5 mm radius opening in the skull bone (facing the incoming blast wave).

In Figure 6.1 we compare the result from the simulations with and without openings. It is clear that the opening hardly influences the pressure inside the brain at all. The tendency was similar in other gauges in the brain (not shown). This leads to the conclusion that the blast wave propagates directly through the skull. This is in agreement with results obtained in (11).

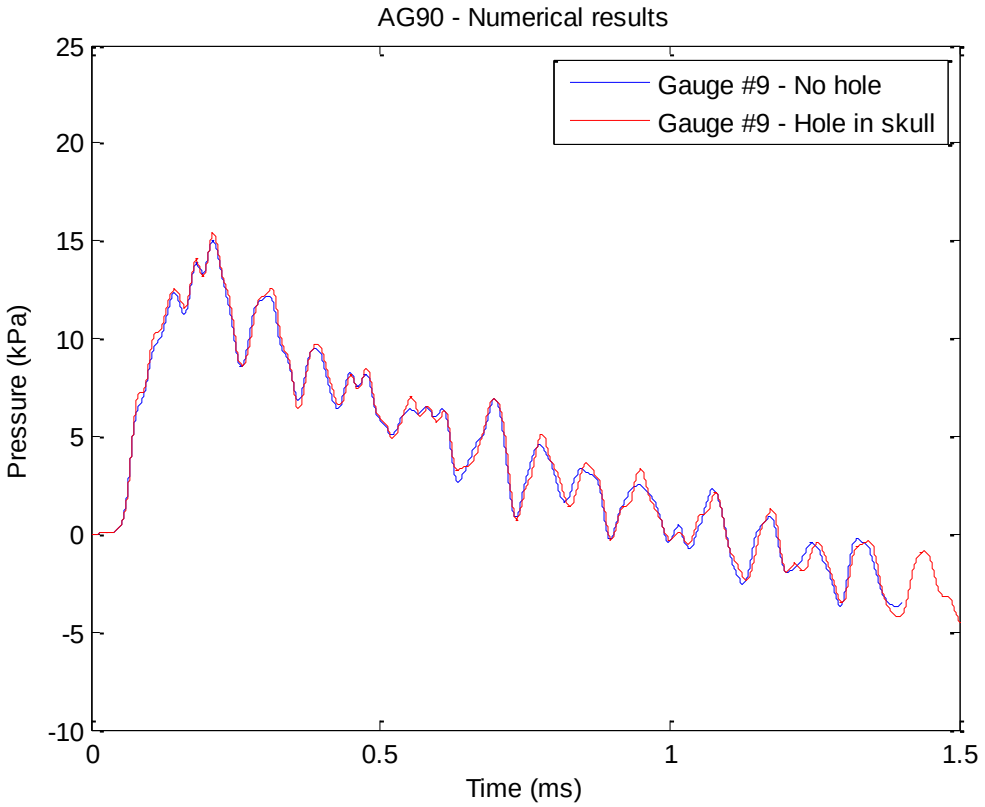

Figure 6.1 AG 90 – With and without opening in the skull bone.

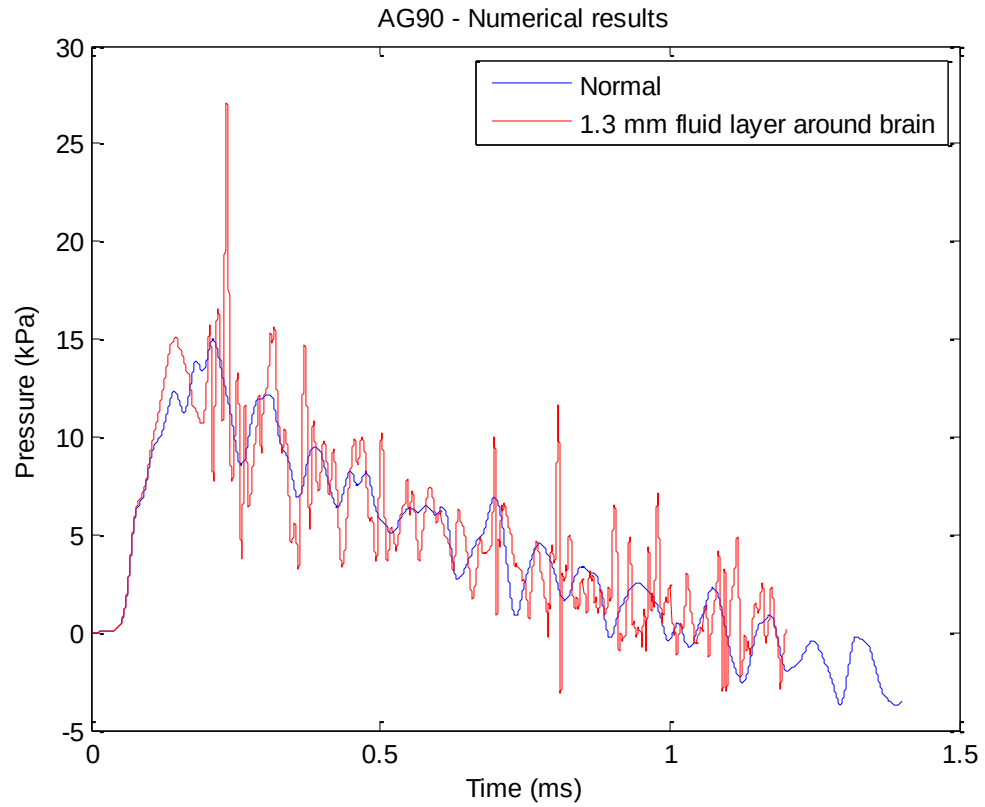

Figure 6.2 AG90: Results with a fluid layer between skull and brain.

6.1 Cerebrospinal Fluid (CSF)

To simulate the presence of CSF, a 1.3 mm thick layer of water (material model taken from the AUTODYN material library) was added between the skull bone and the brain. The results are shown in Figure 6.2. The fluid introduces some oscillations and spikes into the pressure history, but otherwise it has little quantitative influence.

6.2 Influence of head geometry

The numerical results show that the pressure in the brain is highest in the region facing the incoming blast wave. Without going to full 3D, we can only model the case where the head is turned 90 degrees (Figure 6.3).

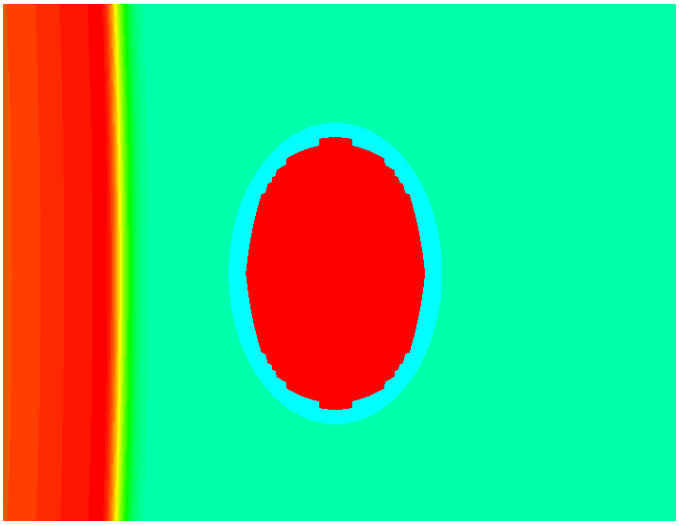

Figure 6.3 Rotated head.

The pressure contours at different points in time for the rotated head are shown in Figure 6.4. In Figure 6.5 we have compared the pressure as a function of time in the centre point of the brain. We note that the changed geometry results in oscillations of much larger amplitude. The total picture is quite complex because of the blast wave scattering around the head and entering through the skull bone from different locations, but these major oscillations can be traced back to waves going back and forth in the head, entering through the skull bone at one side and then reflecting back at the brain-bone interface at the opposite side.

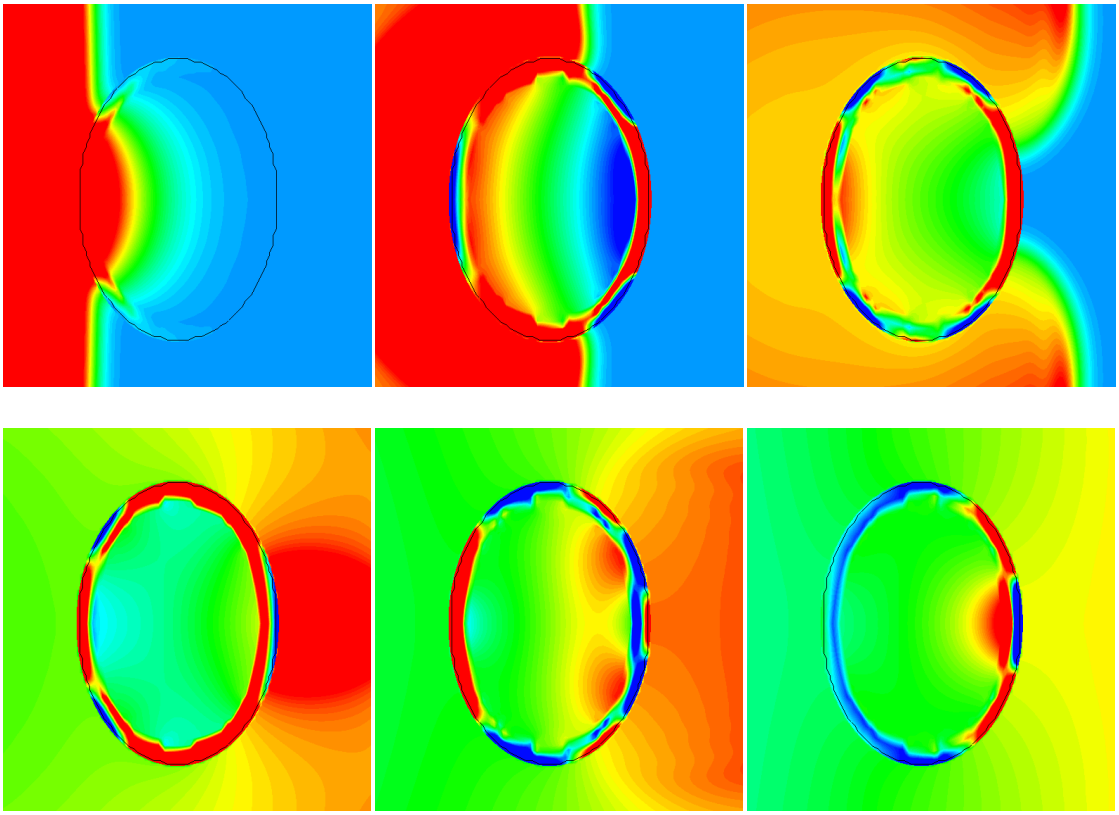

Figure 6.4 Pressure propagation in the rotated head. (0.3 ms between each plot)

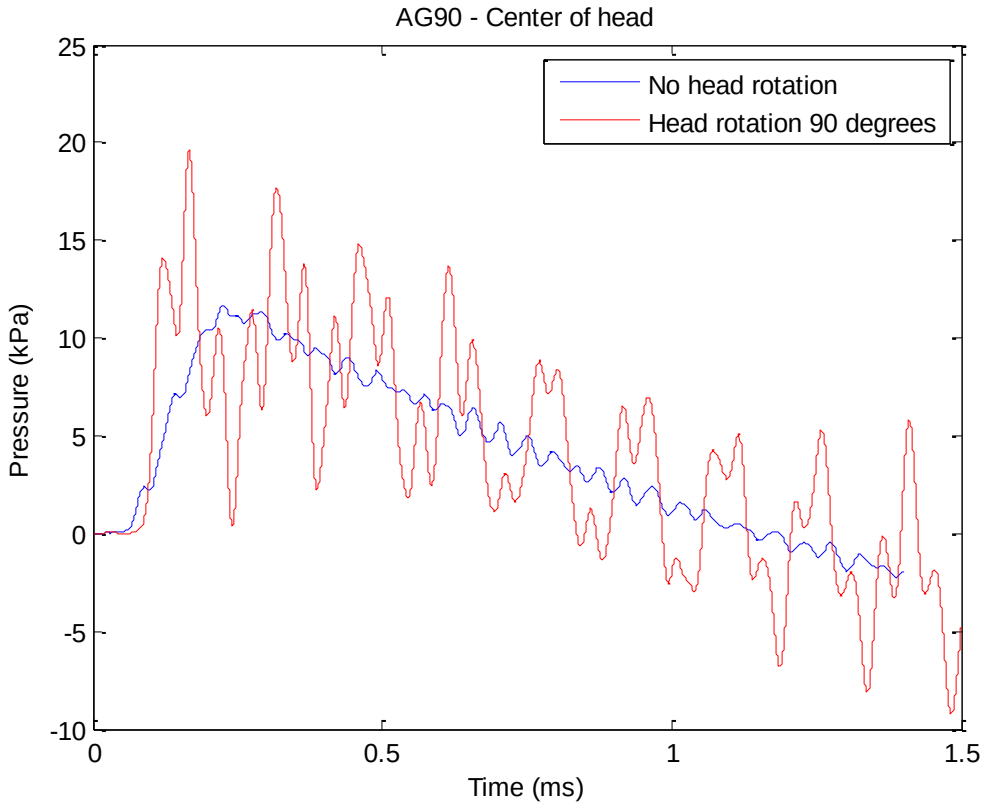

Figure 6.5 Pressure history in the center point for pig head with and without 90 degrees rotation.

6.3 Summary of validation study

Simulations have been performed with a simplified numerical model for the investigation of mechanisms of blast wave propagation into the pig brain. The results were in good agreement with real live experiments on anaesthesized pigs.

Sensitivity studies were performed to establish which parameters are most important for the wave propagation into the brain. It was found that the blast wave propagates into the brain directly through the skull bone. The general size and shape of the blast wave is not affected by openings in the bone. The material parameters of the skull bone are too similar to those of the brain to offer much protection.

7 3D simulations of the blast wave propagating through the human brain

As mentioned earlier, our goal is to study blast waves from a typical IED into the human brain. Since the human skull is not spherically symmetric, this requires numerical simulations in 3D. Instead of going straight to IED blast simulations, we will begin by examing the propagation of the same blast waves from AG90 and FH77 through the human brain to check that the 3D and 2D results are consistent.

7.1 CAD model

For the head geometry for 3D-simulations of blast waves into the brain, a 3D CAD model of the entire human body was purchased from Zygote (12). Special thanks to Bendik Sagsveen who made the necessary transformation of the CAD-file so that it could be imported into AUTODYN.

7.2 Meshing

Using SolidWorks, the head (skull and brain) was extracted from the model and meshed. For the cases with symmetric impact of the blast wave, a model with only half the head was used. This is shown in Figure 7.1.

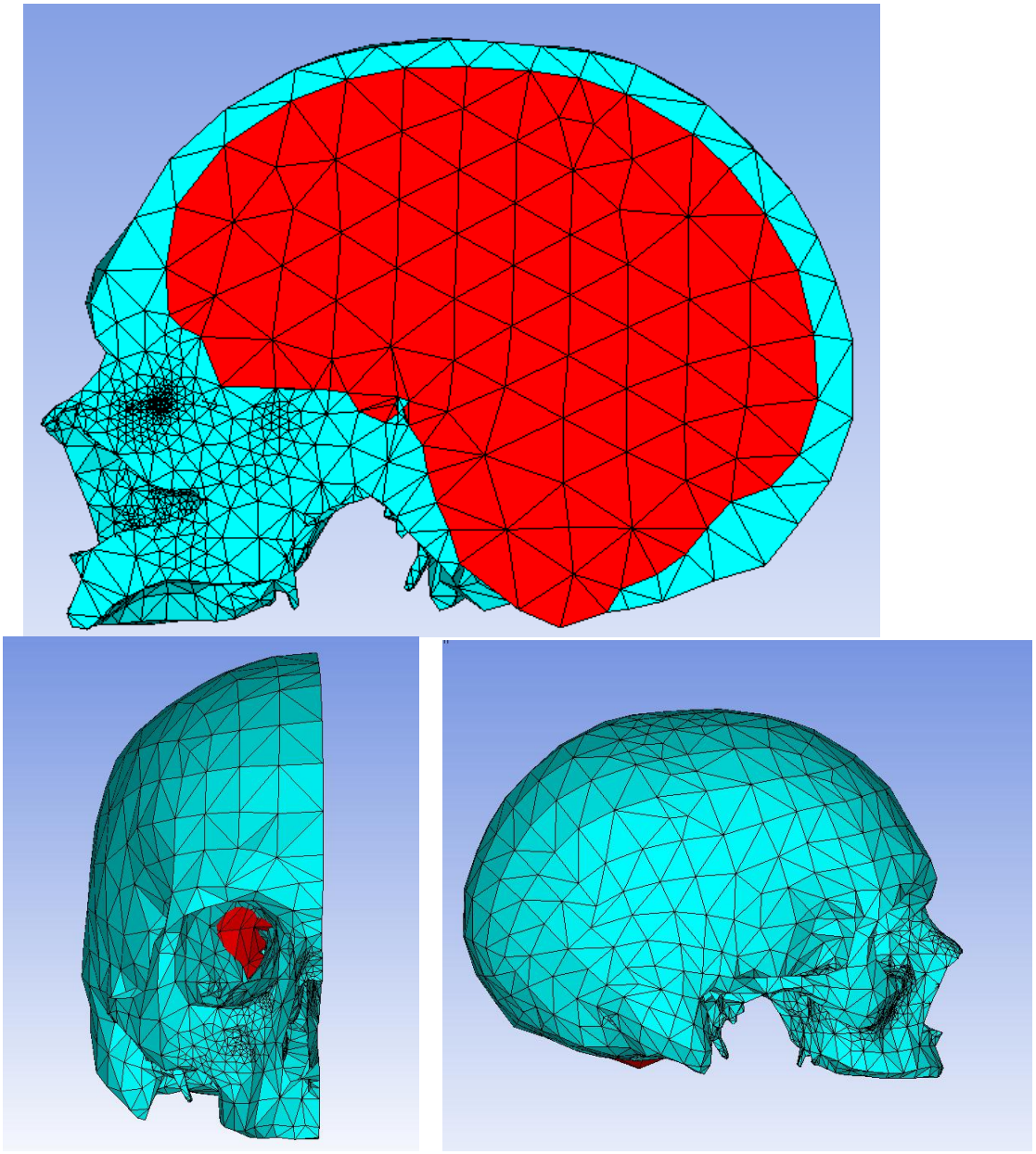

Figure 7.1 Symmetric CAD-model for the skull and brain from various viewing angles.

Due to some very thin surfaces in the skull, some cells in the mesh had very small dimensions (as is seen in the figure. This is a potential problem which can lead to small timesteps and consequently long runtimes, since it is the smallest cell dimension in the geometry which controls the timestep according to the CFL-condition.

AUTODYN has a mechanism called mass scaling for dealing with such situations. This means that small cells can artificially be given extra mass, which lowers the sound velocity for that cell so that it does not control the timestep for the entire simulation. One has to be careful using such an approach, and make sure that the mass scaling does not alter the physical results. In our case the problematic grid cells are all gathered in specific parts of the skull, whereas the brain mesh is okay. In general we are not too interested in the skull, so mass scaling should not be a problem, except if it completely alters the propagation of waves in the skull, which is unlikely in this case.

In the simulation we therefore used automatic mass scaling (with a maximum scaling factor of 100), enabling us to significantly lower the timestep.

No sensitivity study of the mesh size was performed in 3D since 2D results indicated that the results were not very mesh sensitive and the mesh resolution was already as fine as practically possible for numerical simulations.

7.3 Simulation description

The area around the head was modelled using an Euler-Godunov grid. The Godunov processor in AUTODYN is 2nd order in 3D and therefore more accurate than in 2D. A grid size of 10 mm was used. Further, the "flow out" boundary condition was used on the Euler grid to avoid unwanted reflections from the grid edges returning to the head. Note that the absence of the rest of the body allows the waves to enter from below the head as well, whereas the situation would have been more complicated if the waves had to first propagate through the human body. However, as a first approach, this should still give us a good indication of the stress picture inside the brain.

We used the same AG90 and F77 input as in the 2D-simulations, i.e. from spherical TNT charges with similar pressure waves to the real weapons. Gauge points were placed on the symmetry axis of the brain at various locations. The initial state of the 3D-simulation for AG90 is shown in Figure 7.2. Computation time was around three days for 3.0 ms.

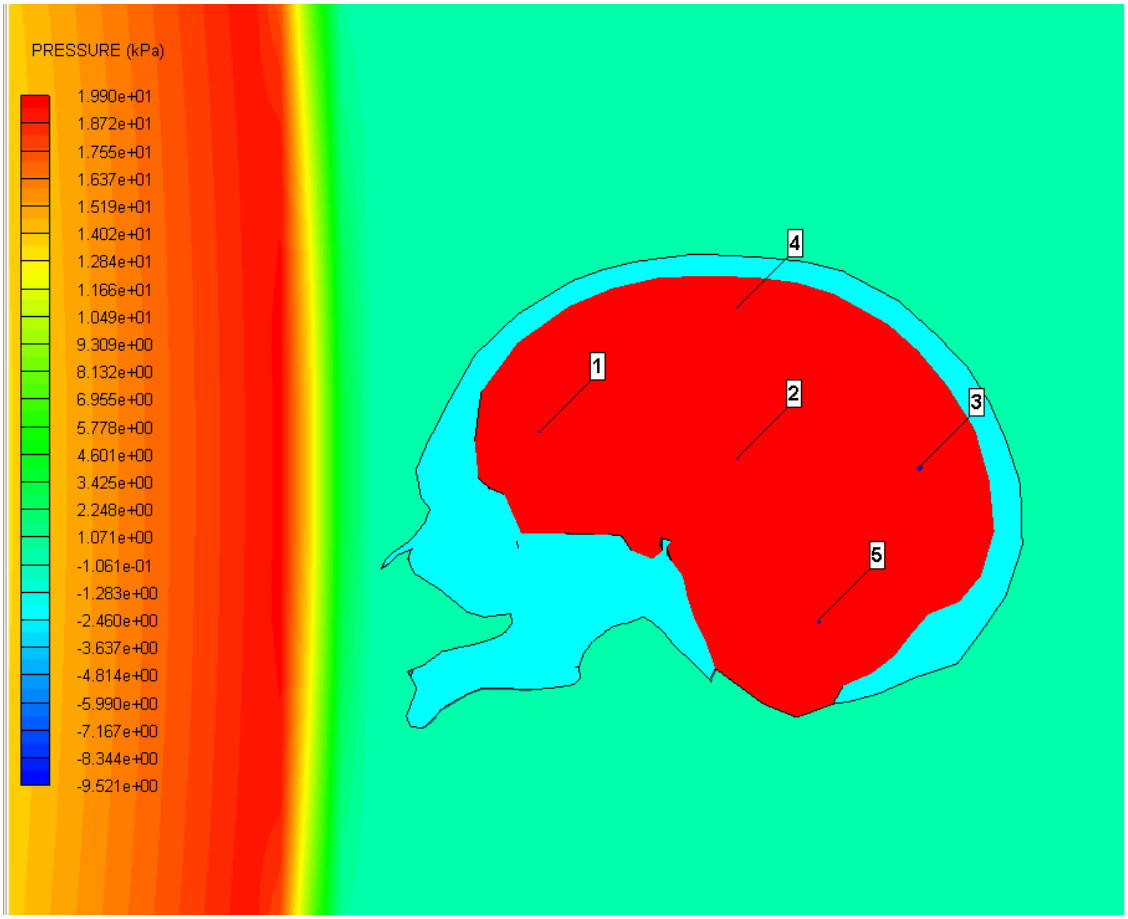

Figure 7.2 Initial state of the 3D-simulation after remapping from 1D.

7.4 AG90 results

The new simulations now enable us to see how the blast wave propagates into the head. In Figure 7.3 a contour plot of the skull surface is shown, whereas Figure 7.4 shows the brain through a cross section of the skull.

The numerical results for pressure at the different gauge points in the brain, compared with the free field pressure, are shown in Figures 7.5 and 7.6.

We see that the features of results are consistent with the 2D simulation results as well as the experimental results for pigs. However, the 3D results give us a slightly more refined picture of how the blast wave propagates inside the brain (and skull).

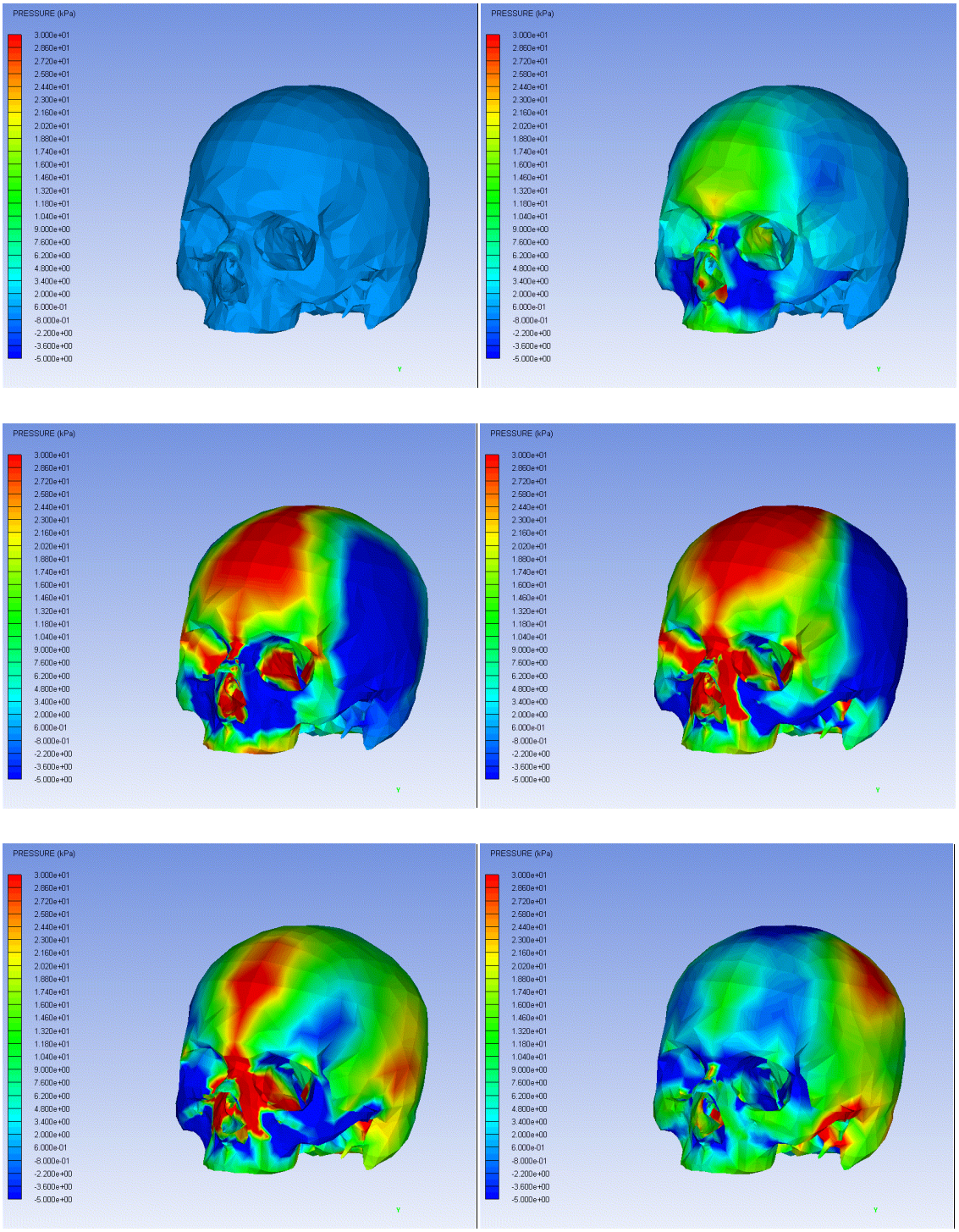

Figure 7.3 Propagation of the blast wave into the head

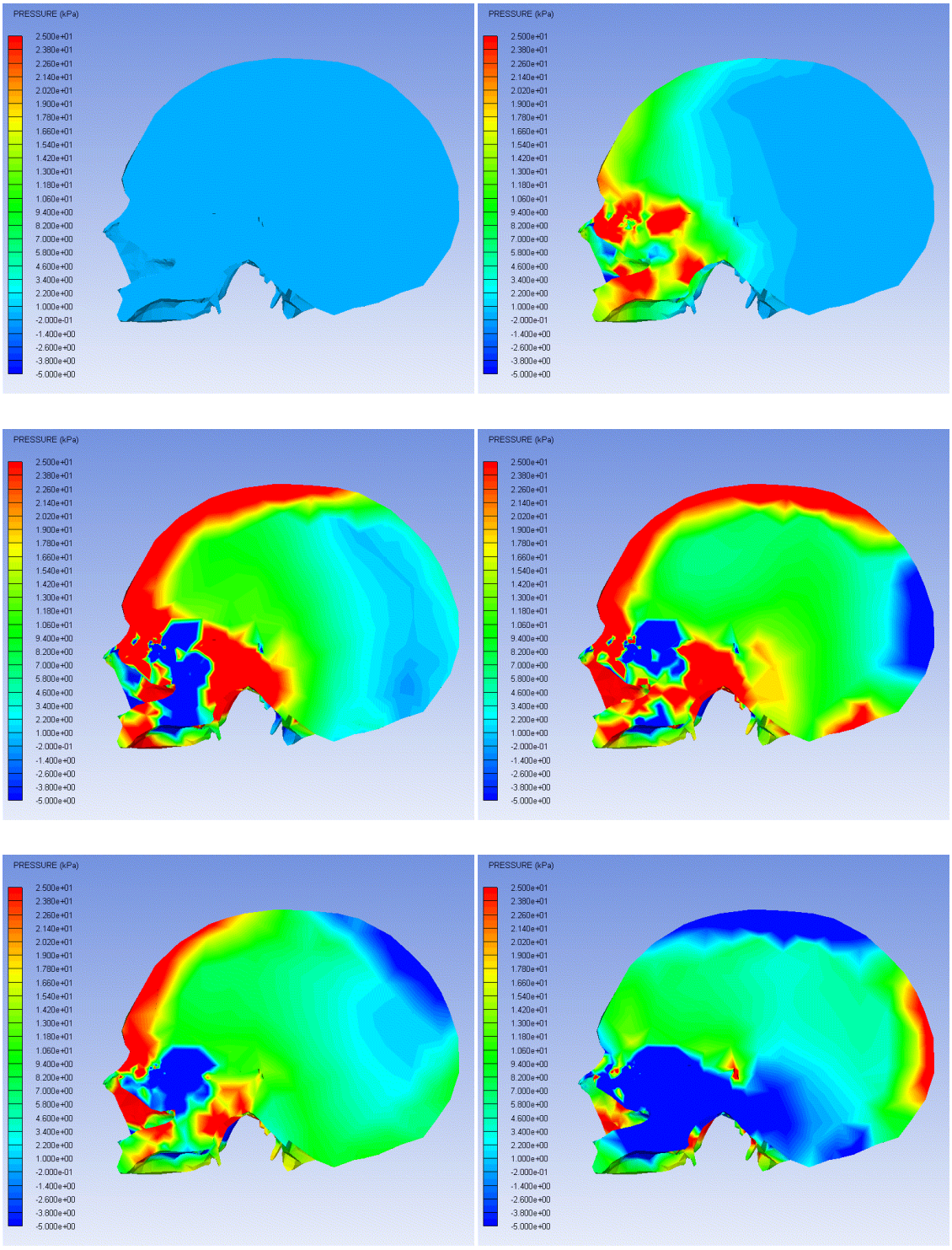

Figure 7.4 Propagation of the blast wave into the head (cross-section through center)

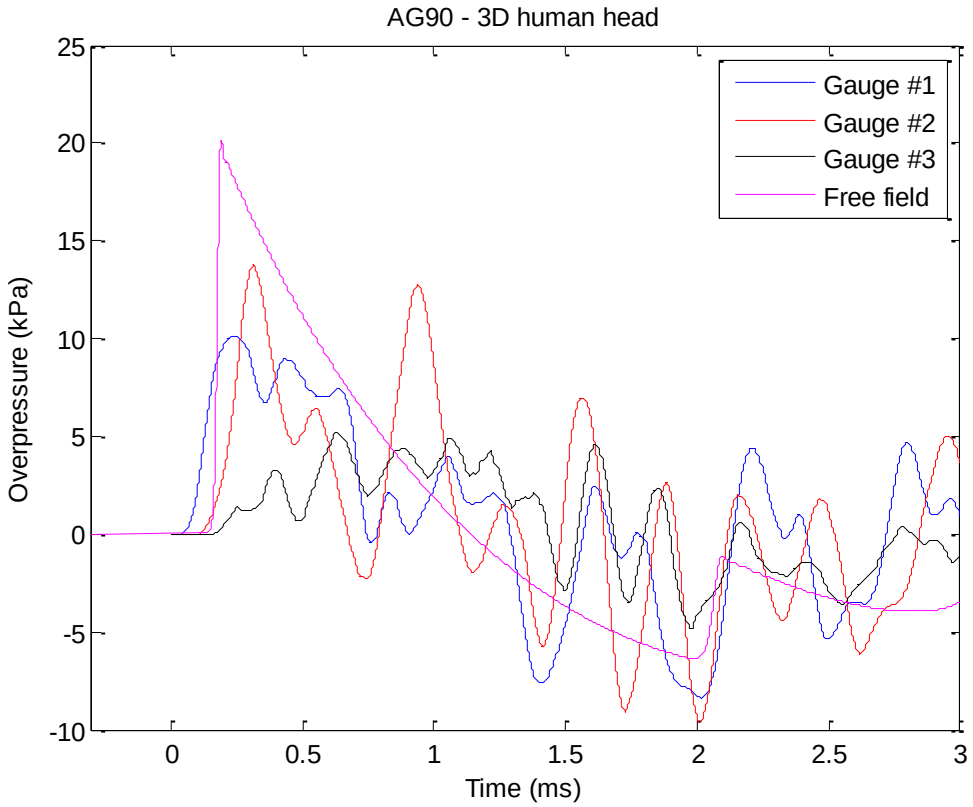

Figure 7.5 Pressure in brain for AG90 case compared to free field

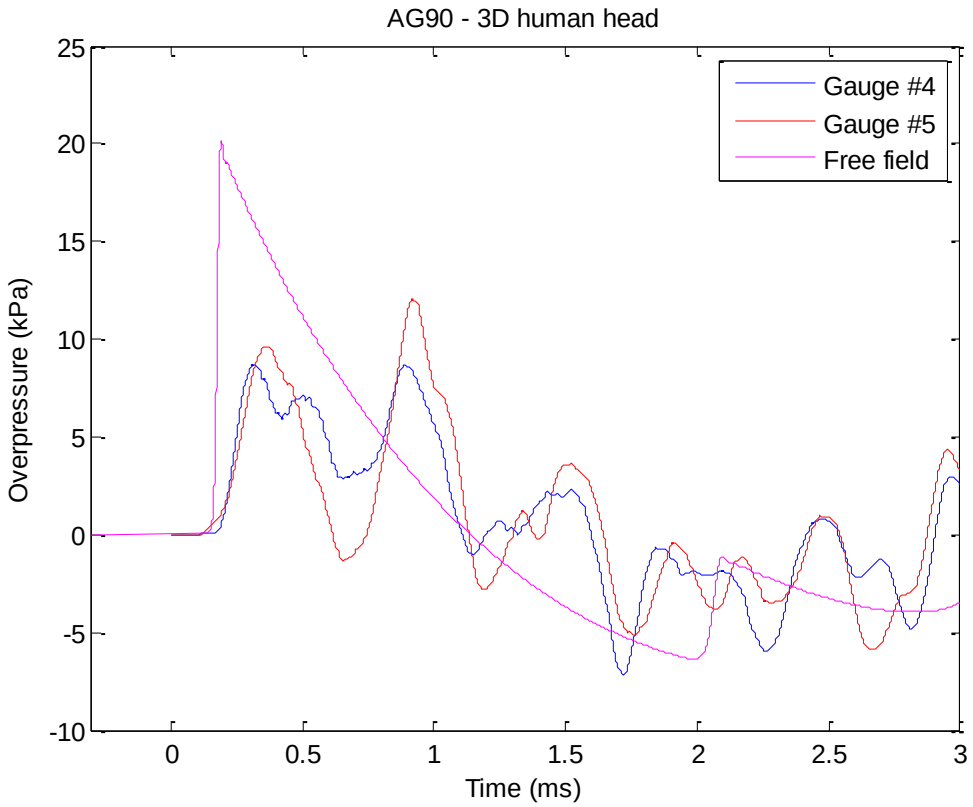

Figure 7.6 Pressure in brain for AG90 case compared to free field

In the 3D-simulations we can rotate the head in any direction we want. For example, it can be interesting to see how the results differ when the blast wave enters from the rear of the head instead of the front. This is shown in Figures 7.7 and 7.8 for two of the gauge points.

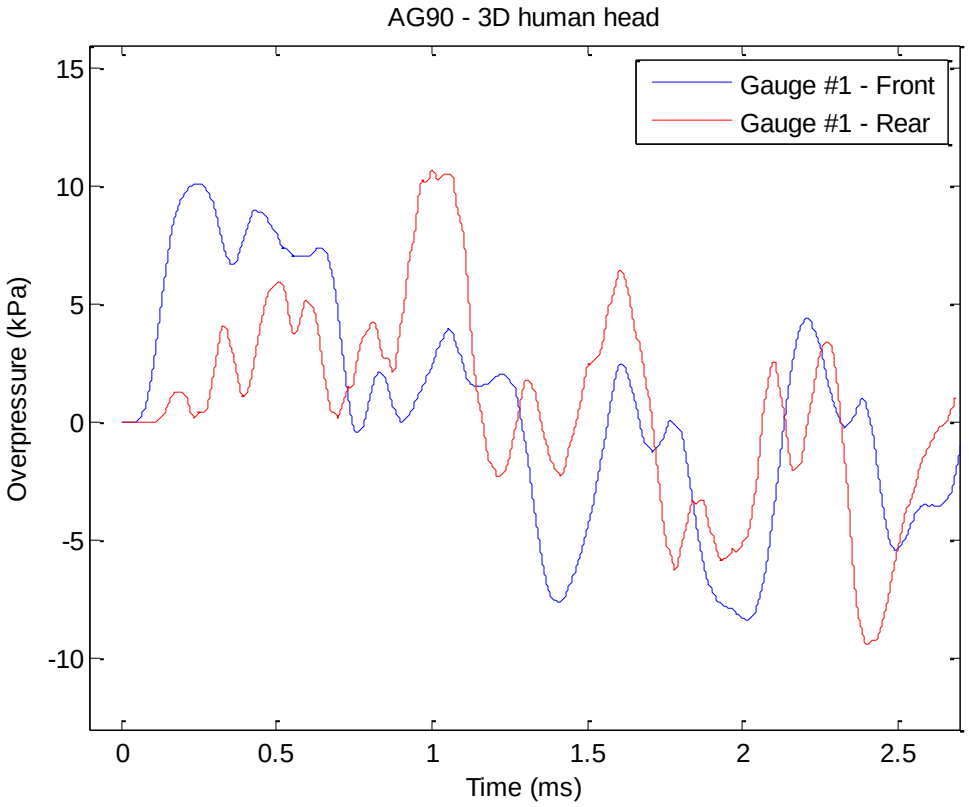

Figure 7.7 Comparison between pressure in brain depending on whether the blast wave enters from the front or the rear of the head.

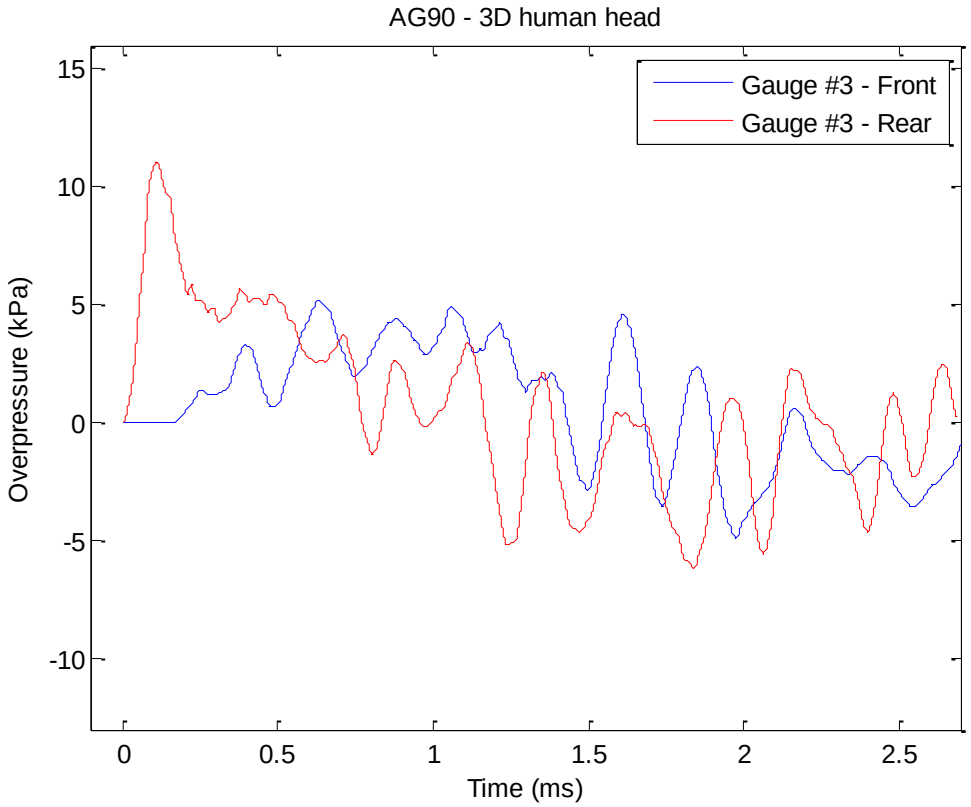

Figure 7.8 Comparison between pressure in brain depending on whether the blast wave enters from the front or the rear of the head.

7.5 FH77

For FH77 the results are obtained in the same way and shown in Figures 7.9-7.12. Again the results are consistent with 2D results and experiments.

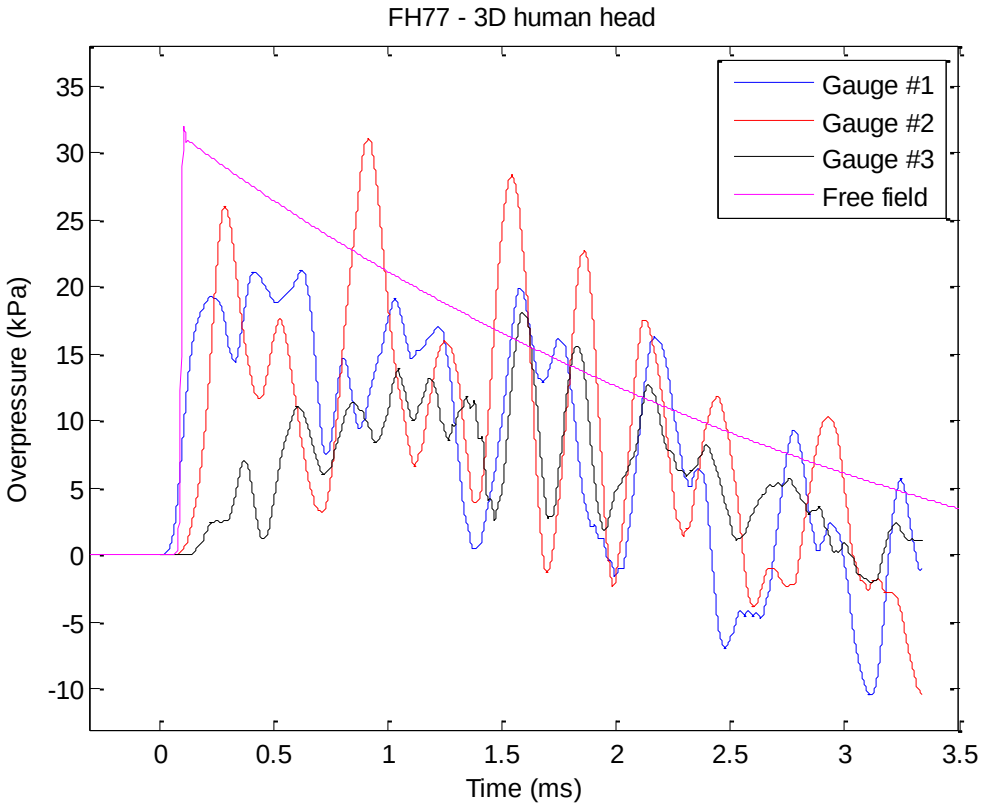

Figure 7.9 Pressure in brain for FH77 case compared to free field

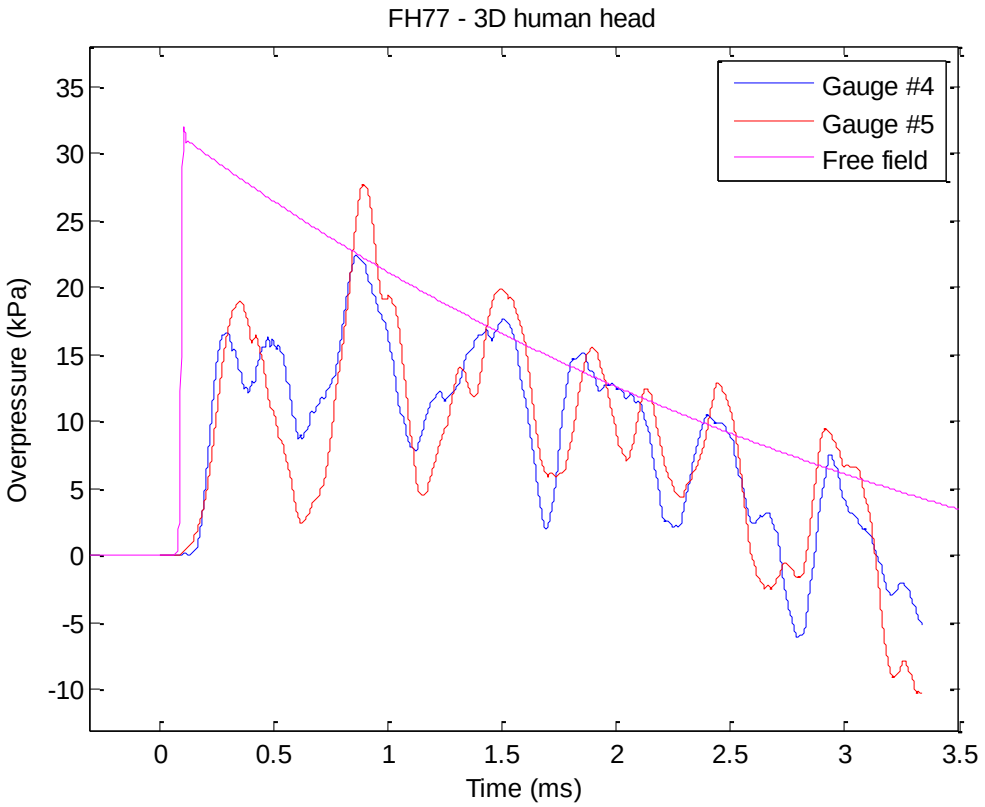

Figure 7.10 Pressure in brain for AG90 case compared to free field

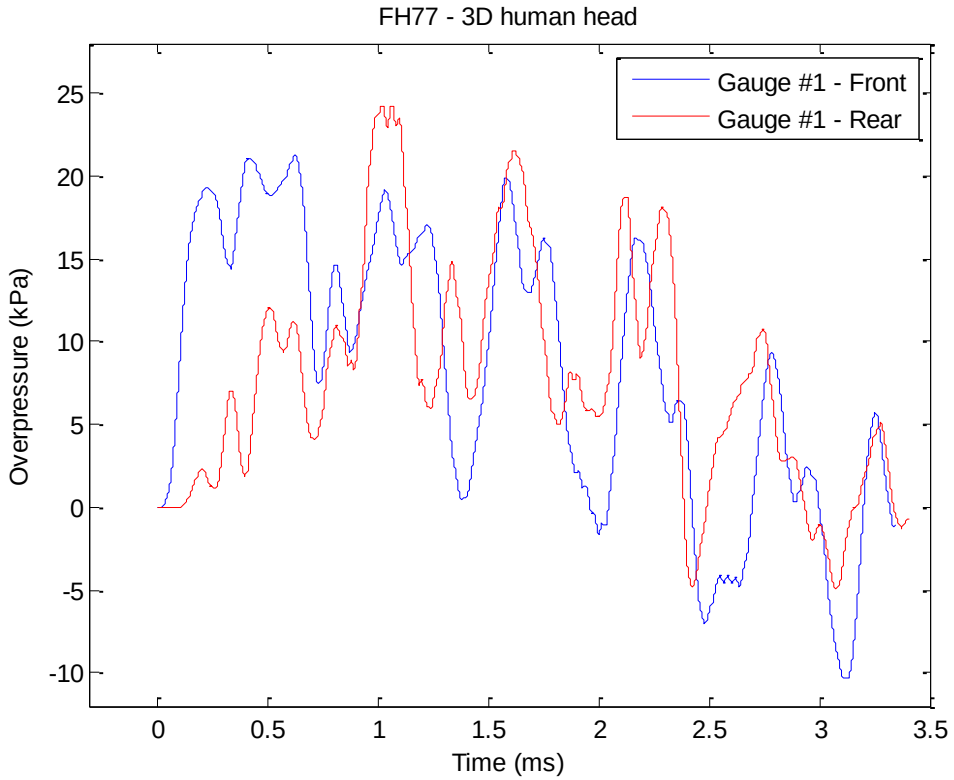

Figure 7.11 Comparison between pressure in brain depending on whether the blast wave enters from the front or the rear of the head.

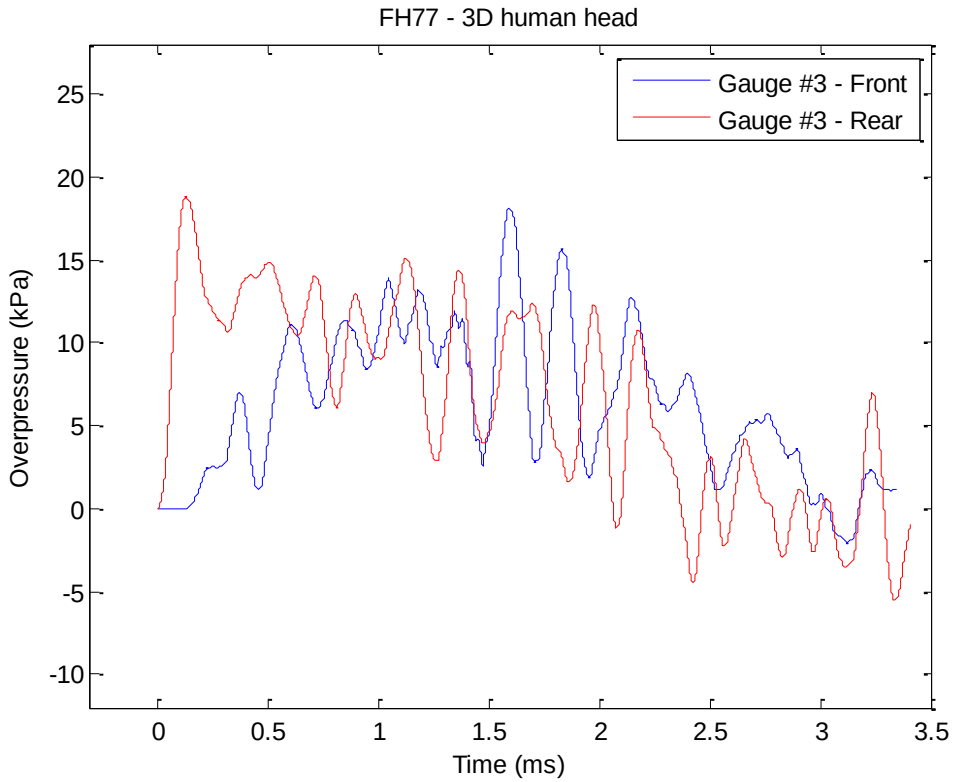

Figure 7.12 Comparison between pressure in brain depending on whether the blast wave enters from the front or the rear of the head.

7.6 Summary of 3D modelling

Summing up the results from the 3D numerical simulations, we see that:

- The blast wave is practically not dampened by the skull
- The blast wave propagates directly through the skull and is not dependent on propagating through the openings in the scull (nose, ears, eyes, throat)
- The orientation of the blast relative to the head has effect on blast pressure in the brain
- In general the full 3D results are consistent with the 2D results.

We now turn our attention to the propagation of blast waves from an IED into the brain. The main difference is that these will have higher amplitude than the blast waves from the weapons.

8 IED

As an example of an IED, we study a 7.5 kg bomb of "homemade explosives" at a distance of 4.5 m. AUTODYN does not have a material model for such an explosive, but the pressure wave from such a bomb was seen to be almost equal to a 4 kg TNT charge at 4.80 meters distance, so this was the actual case studied. In Figure 8.1 we show the measured pressure history from the homemade bomb together with the AUTODYN simulation with TNT.

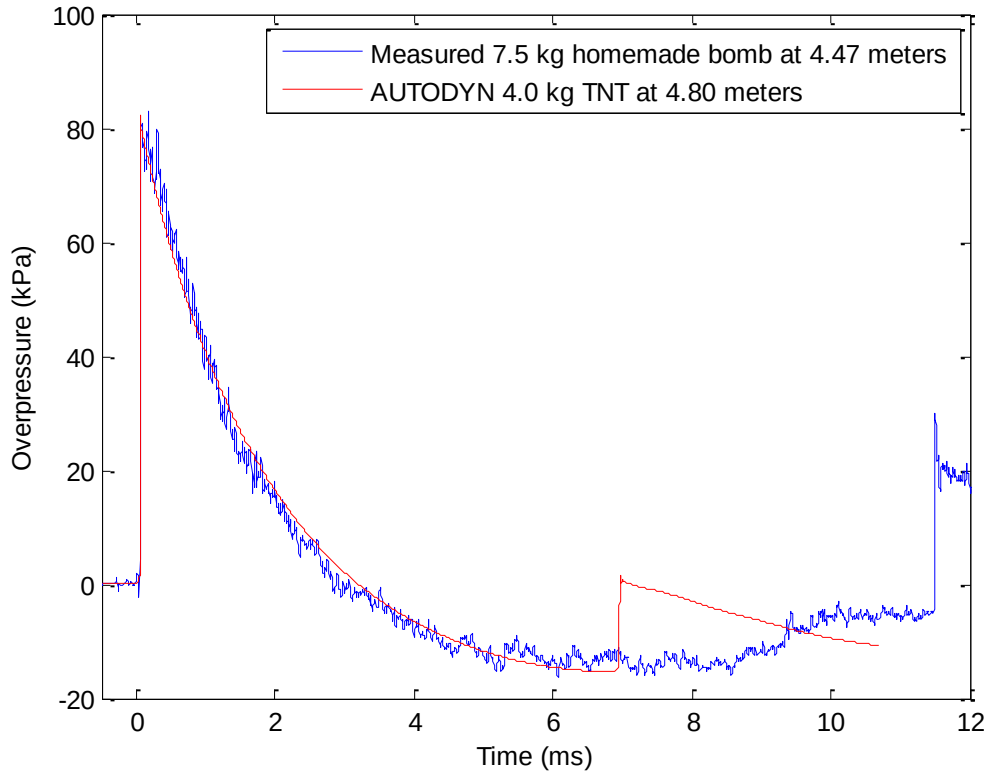

Figure 8.1 Comparison between measurements with homemade bomb and AUTODYN simulations using TNT.

The agreement is extremely good for the first 7 ms. The only difference is that the secondary wave for TNT comes much earlier than for the homemade bomb. However, the initial wave will do most of the damage, justifying the use of TNT as the source in the simulations.

Simulations were performed to see how this blast wave would propagate into the skull. To generate the incident wave, a 1D spherical simulation was performed for the first 4.80 meters until the wave reached the skull. The 1D final state was then remapped to a 3D simulation. The initial state of the 3D-simulation in shown in Figure 8.2.

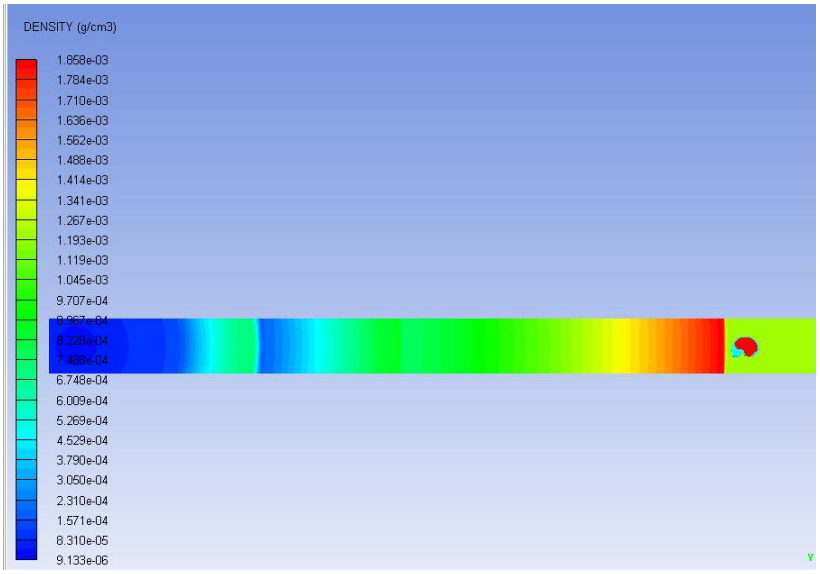

Figure 8.2 Initial state of the 3D simulation of an IED blast wave propagating into the human head.

Due to the large distance from the charge (and consequently very long duration blast wave), a very large grid is needed. Flow out boundary conditions are used in the y- and z-direction. These seemed to work fine and no unwanted reflections were found.

The gauges were in the same position as in the AG90 and FH77 simulations. The results are shown in Figures 8.3-8.4. We note that the pressure amplitudes inside the brain in some locations are roughly comparable with the free field amplitudes. However, the pressure amplitudes depend quite a lot on position. Further, we see that pressure oscillations with very high amplitudes are generated inside the brain. The nature of these oscillations depend on the material properties of the brain. If we had used a viscoelastic model instead of a purely elastic model, these would have been damped more quickly.

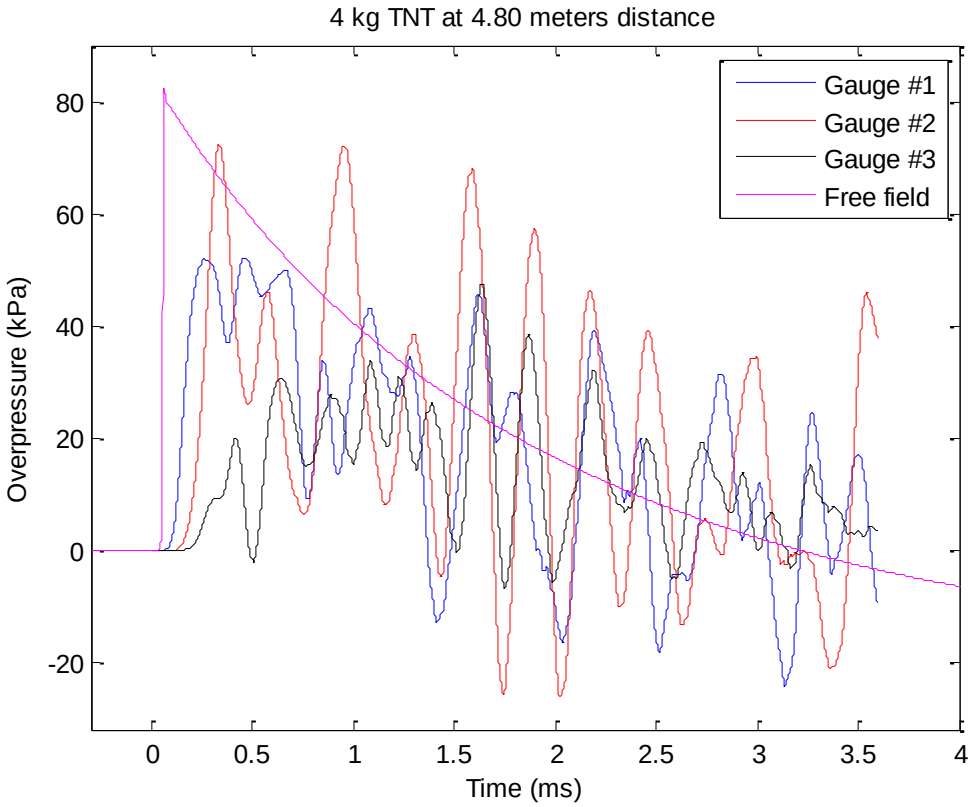

Figure 8.3 Pressure in brain for an IED blast wave compared to free field

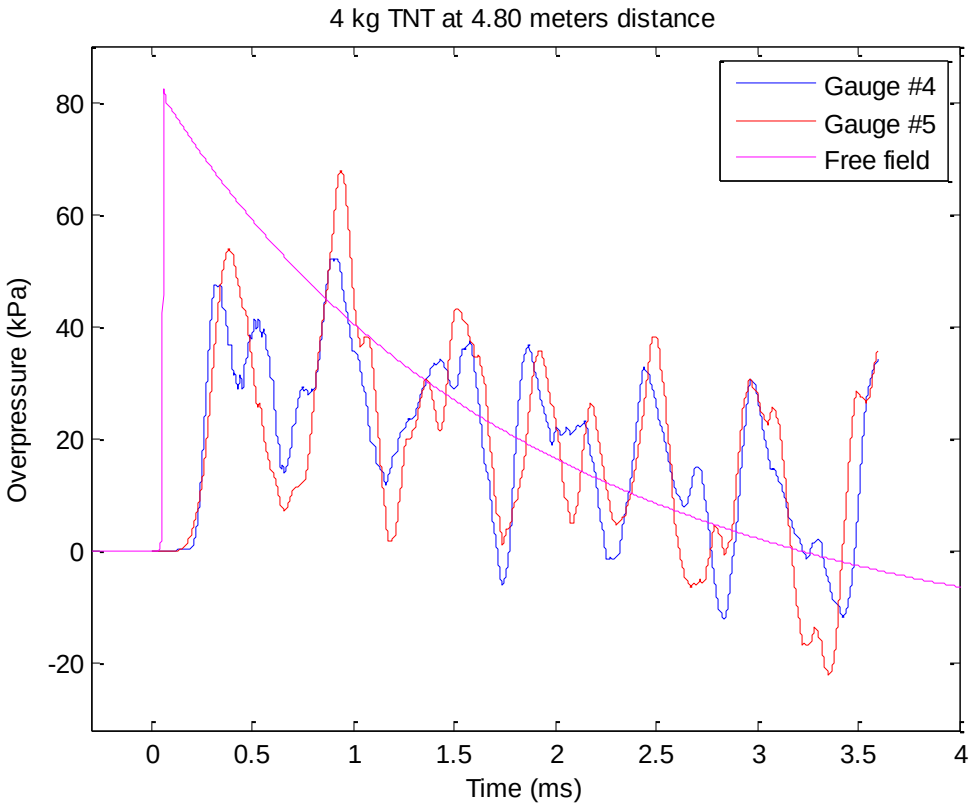

Figure 8.4 Pressure in brain for an IED blast wave compared to free field

9 Summary

Blast induced TBI from IED's and mTBI from training with heavy weapons and explosives is a new field with many unresolved problems. In this report we have shown how to simulate blast waves propagating through the brain, and used these simulations to explore some of the fundamental mechanisms.

Simulations were first performed with a simplified numerical 2D model for the investigation of mechanisms of blast wave propagation into the pig brain. This allows for shorter computation time and makes it possible to perform parameter studies. The results were in good agreement with real live experiments with pressure sensors in the brain of anaesthesized pigs. The blast waves were taken from experiments that induced hemorages in the pigs brains. Similar strength blast waves temporally reduce cognitive capabilities in rats.

Sensitivity studies were performed to establish which parameters are most important for the wave propagation into the brain. It was found that the blast wave propagates into the brain directly through the skull bone. The general size and shape of the blast wave is not affected by openings in the bone (nose, ears, eyes, throat). The material parameters of the skull bone are too similar to those of the brain to offer much protection.

Having validated the 2D numerical model, we performed simulations with 3D CAD geometry of a human head. We performed simulations studying the propagation of blast waves from a homemade IED into the brain. Again the results showed that the skull offered little protection. The blast wave is practically not dampened by the skull. The blast wave propagates directly through the skull and is not dependent on openings in the skull to propagate into the brain. The orientation of the blast relative to the head has effect on blast pressure in the brain. In general the full 3D results are consistent with the 2D results.

In most of the simulations we see large oscillations behind the first peak. Such oscillations correspond well to how blast waves may propagate back and forth in the brain and scull, given the chosen material model. It seems however plausible that these oscillations would be damped in real brain tissue. The first peak would probably be the same, but the oscillations may die out faster. Further work may include improving the material models for brain tissue to incorporate damping at the relevant time and length scales.

In total we now have a validated (but simplified) numerical method for studying the pressure propagation and other physical parameters inside a human head exposed to a blast wave. This could be helpful in further exploring the mechanisms that possibly lead to brain injury, both from "weak" shock waves from weapons or from "strong" shock waves from an IED.

References

(1) Säljö A, Bolouri H, Mayorga M, Svensson B, Hamberger A, Low-level blast raises intracranial pressure and impairs cognitive functions in rats, Journal of Neurotrauma, 2009 Mar 24

(2) Huseby M, Opstad P K, Svinsås E. Forprosjekt: Faren for hjerneskader hos personell som benytter Forsvarets våpen og eksplosiver. FFI-notat 2009/01062, 2009

(3) Teland J A, Hamberger A, Huseby M, Säljö A, Numerical simulation of mechanisms of blast-induced traumatic brain injury, Journal of Acustic Society America, Volume 127, Issue 3, p. 1790, 2010 (Proceedings of Meetings on Acoustics, Vol 9, 020004, 2010)

(4) Teland J A, Hamberger A, Huseby M, Säljö A, Numerical simulation of blast induced mild traumatic brain injury, Proceedings of 6th World Congress on Biomechanics, Singapore, 1-6 august 2010

(5) Säljö A, Arrhén F, Bolouri H, Mayorga M, Hamberger A (2008), Neuropathology and pressure in the pig brain resulting from low-impulse noise exposure, Journal of Neurotrauma 25:1397-1406, 2008

(6) www.ansys.com

(7) Teland J A, Rahimi R, Huseby M, Numerical simulation of sound emission from weapons, Proceedings of the 35th Inter-Noise conference, Hawaii, USA, 3-6 december 2006

(8) Teland J A, Rahimi R, Huseby M, Numerical simulation of sound emission from weapons, Noise Control Engineering Journal, Vol. 55, No. 4, 2007

(9) Anderson R D, Fickie K D, IBHVG2 – A User's guide, Ballistic Research Laboratory, Aberdeen, USA

(10) Cowin S C, Bone Mechanics handbook 2nd edition, Informa Healthcare, 2001

(11) Moss W C, King M J, Blackman E G, Skull Flexure from Blast Waves: A Mechanism for brain injury with implications for helmet design, Physical Review Letters 103, 108702, 2009

(12) www.zygote.com